Current Biology, Volume *32*

Supplemental Information

Reprogramming the topology of the nociceptive circuit in *C. elegans* reshapes sexual behavior

Vladyslava Pechuk, Gal Goldman, Yehuda Salzberg, Aditi H. Chaubey, R. Aaron Bola, Jonathon R. Hoffman, Morgan L. Endreson, Renee M. Miller, Noah J. Reger, Douglas S. Portman, Denise M. Ferkey, Elad Schneidman, and Meital Oren-Suissa

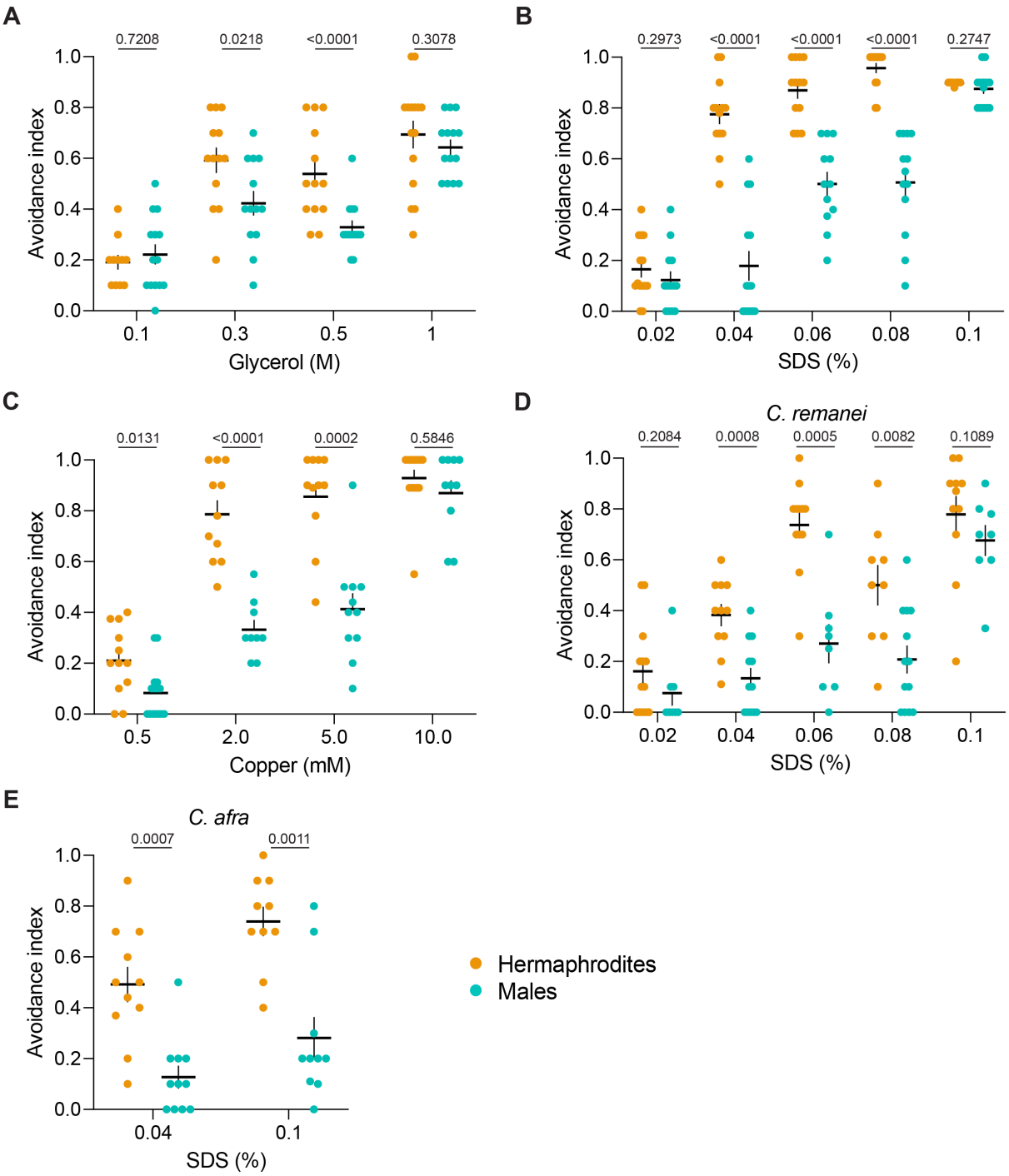

Figure S1. Behavioral responses of individual animals to multimodal nociceptive stimuli, Related to Figure 1

(A-C) Individual animals represented by dots, see averages in Figure 1C-E. (D-E) Individual animals represented by dots, see averages in figure 1G-H. Horizontal lines represent the means and vertical lines represent the SEM. We performed a Mann-Whitney test for all comparisons.

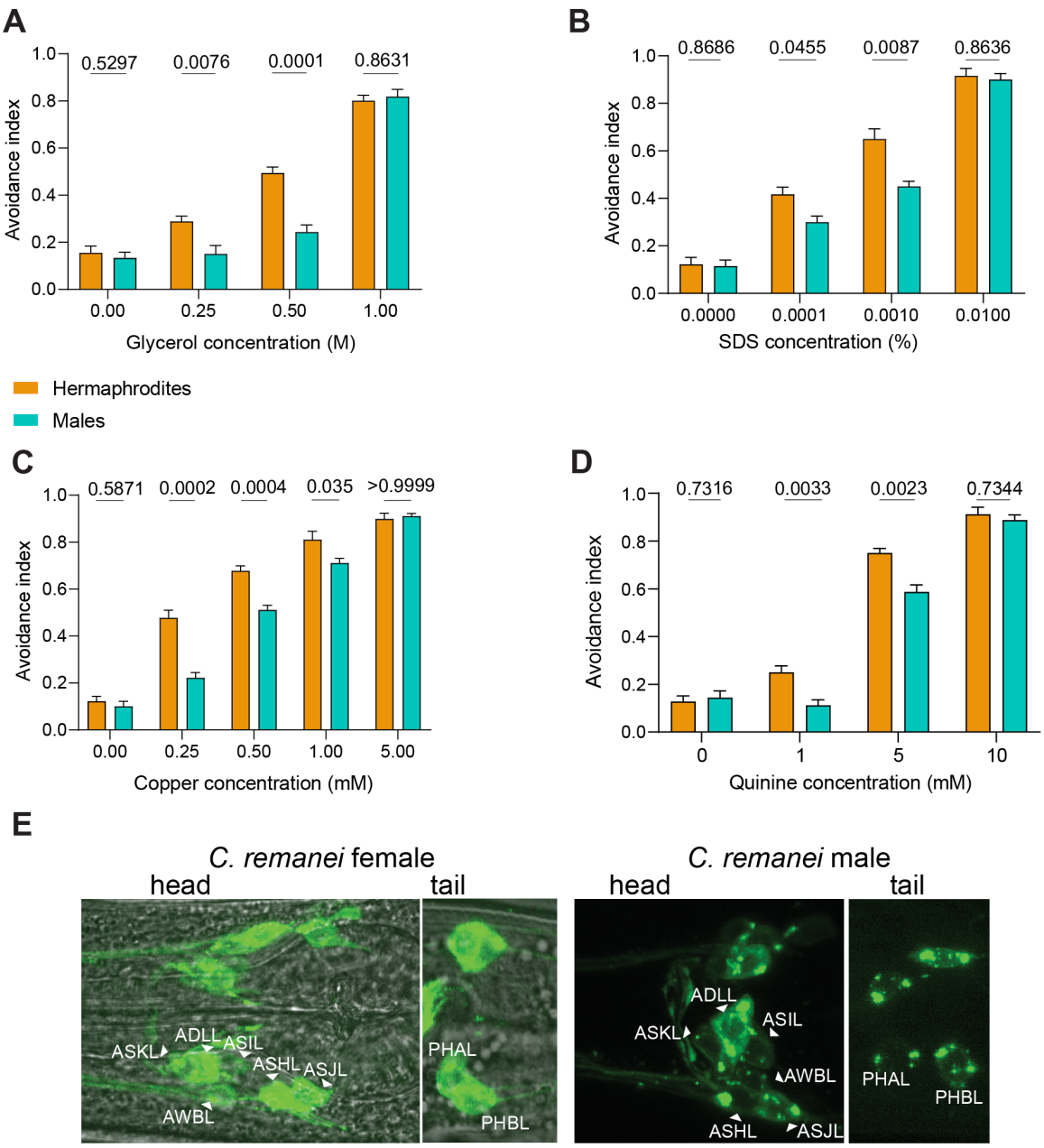

Figure S2. Sexually dimorphic avoidance behavior to multimodal stimuli, Related to Figure 1

(A-D) Chemosensory repulsion head-drop assays (see Methods for full description). Hermaphrodites reverse more than males at intermediate concentrations of aversive stimuli - glycerol (A), SDS (B), copper (C) and quinine (D). n = glycerol - 9 repeats per concentration, SDS - 6-9 repeats per concentration, copper - 9 repeats per concentration, quinine - 8-9 repeats per concentration. Every repeat was done on ~15 worms per sex. Vertical lines represent the SEM. (E) Representative confocal micrographs of a *C. remanei* female (left) and male (right) stained with the lipophilic dye DiO, showing the same sensory neurons as *C. elegans*, both in the head and in the tail. We performed a Mann-Whitney test for all comparisons.

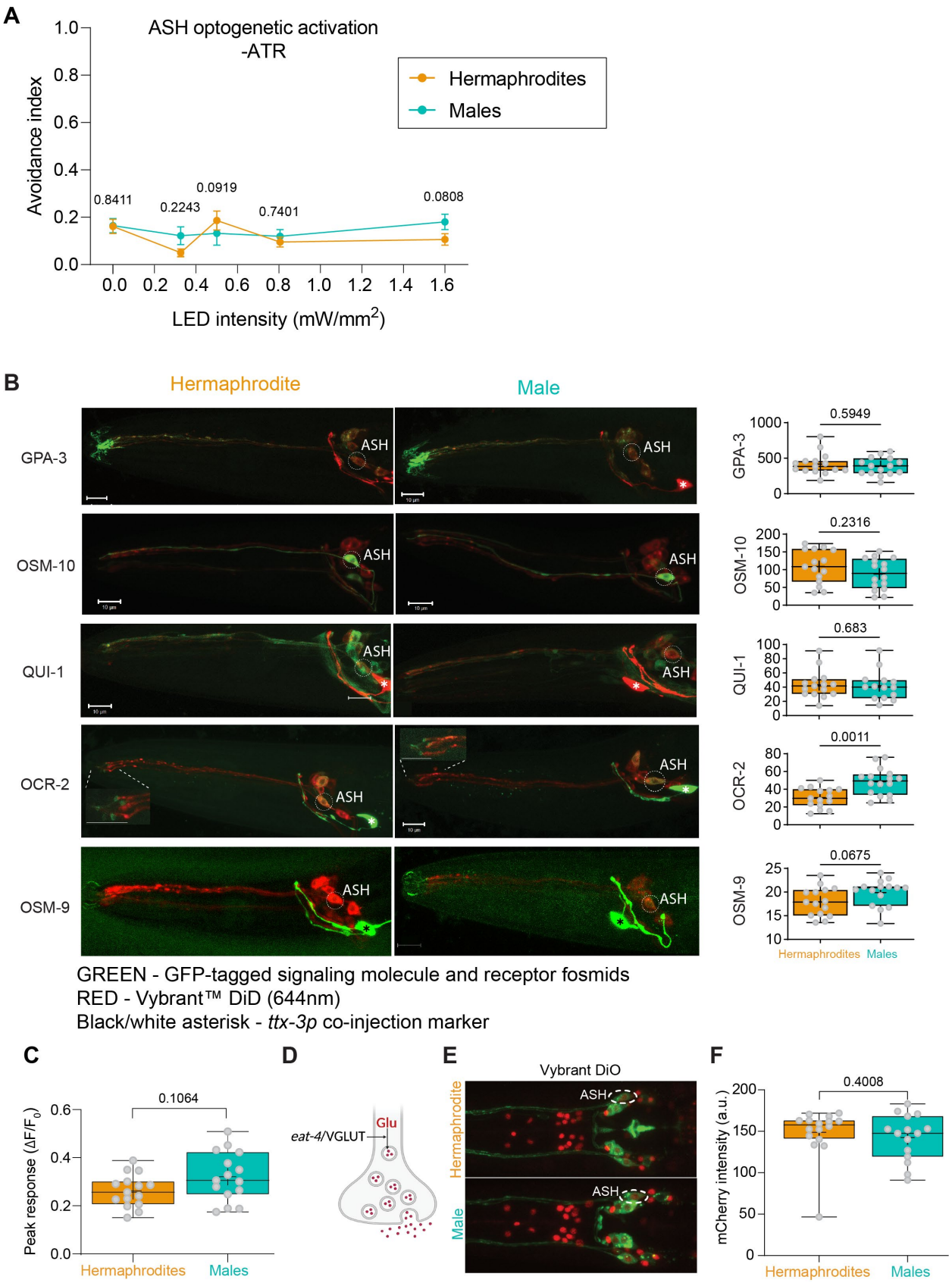
A
ASH optogenetic activation
-ATR
Hermaphrodites
Males
Avoidance index
1.0
0.8
0.6
0.4
0.2
0.0
0.8411
0.2243
0.0919
0.7401
0.0808
0.0 0.2 0.4 0.6 0.8 1.0 1.2 1.4 1.6
LED intensity (mW/mm2)
B
Hermaphrodite
Male
GPA-3
OSM-10
QUI-1
OCR-2
OSM-9
ASH
0.5949
0.2316
0.683
0.0011
0.0675
Hermaphrodites
Males
GREEN - GFP-tagged signaling molecule and receptor fosmids
RED - Vybrant™ DiD (644nm)
Black/white asterisk - ttx-3p co-injection marker
C
0.1064
Peak response (ΔF/F0)
Hermaphrodites
Males
D
eat-4/VGLUT
Glu
E
Vybrant DiO
Hermaphrodite
Male
ASH
F
0.4008
mCherry intensity (a.u.)
Hermaphrodites
Males

Figure S3. ASH senses aversive stimuli similarly in the two sexes, Related to Figure 2

(A) Optogenetic activation experiments of animals without all-trans-retinal (ATR) (control groups for Figure 2D). n = 30-40 hermaphrodites, 29-38 males. (B) On the left, representative confocal micrographs of 1 day adult hermaphrodites and males expressing fosmid reporters of candidate signaling molecules and receptor genes (*gpa-3, osm-10*, *qui-1*, *ocr-2*, *osm-9*) tagged with GFP, and Vybrant lipophilic dye (DiD), enabling ASH identification (marked by white dashed ovals). In *ocr-2* micrographs, the inset is a magnification of the nose, labeling subcellular expression in the dendritic tip. Some images also show the co-injection marker *ttx-3p::mCherry/GFP*. On the right, quantification of the expression levels of the same proteins, measured at ASH soma (see Methods). Y axis in all five graphs is GFP tagged fosmid expression in arbitrary units. n = 14-16 animals per group. (C) Quantification of the peak responses of individual animals' ASH calcium responses (Figure 2E-F). n = 15 hermaphrodites, 15 males. (D) Illustration of protein *eat-4*/VGLUT's function, packaging glutamate into vesicles in neurons. (E) Representative images of *eat-4*/VGLUT protein levels in ASH (marked with dashed circles), in the two sexes. ASH was identified using DiO staining (see Methods). (F) Quantification of *eat-4*/VGLUT fosmid reporter expression in ASH. n = 16 hermaphrodites, 15 males. Scale bars in all confocal micrographs are 10 µm. B, C and F are box and whiskers plots, vertical line represents the median and "+" is the mean. We performed a Mann-Whitney test for all comparisons.

A

ASH / AVB	AVB / AVA	B / A	B / A	# Parameter sets: Behavioral output conditions — Herm.	Males	Overlap	Behavioral conditions (overlap) + additional physiological conditions (hermaphrodites)
Excitation	Excitation	Excitation	Excitation	18782	12149	2667	0
Excitation	Excitation	Excitation	Inhibition	18855	12458	2598	0
Excitation	Excitation	Inhibition	Excitation	18503	12096	2744	0
Excitation	Excitation	Inhibition	Inhibition	18746	12457	2699	0
Excitation	Inhibition	Excitation	Excitation	26976	20050	7363	0
Excitation	Inhibition	Excitation	Inhibition	27061	20303	7344	0
Excitation	Inhibition	Inhibition	Excitation	26852	19902	7405	0
Excitation	Inhibition	Inhibition	Inhibition	26972	19915	7362	0
Inhibition	Excitation	Excitation	Excitation	21737	12163	2613	667
Inhibition	Excitation	Excitation	Inhibition	21836	12355	2541	671
Inhibition	Excitation	Inhibition	Excitation	21591	12085	2594	664
Inhibition	Excitation	Inhibition	Inhibition	21937	12306	2575	659
Inhibition	Inhibition	Excitation	Excitation	31604	19776	7032	891
Inhibition	Inhibition	Excitation	Inhibition	31673	20283	7047	838
Inhibition	Inhibition	Inhibition	Excitation	31445	19811	7214	880
Inhibition	Inhibition	Inhibition	Inhibition	31563	20073	7156	873

Excitation Inhibition

B

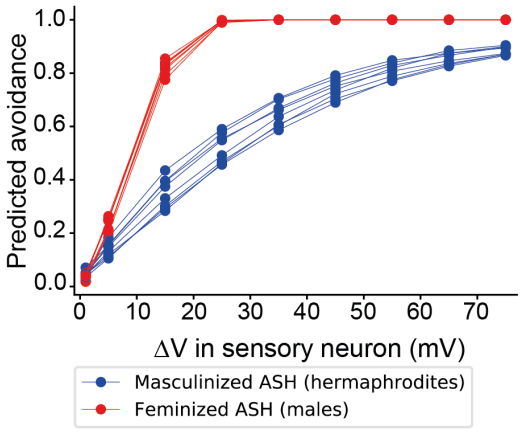

C

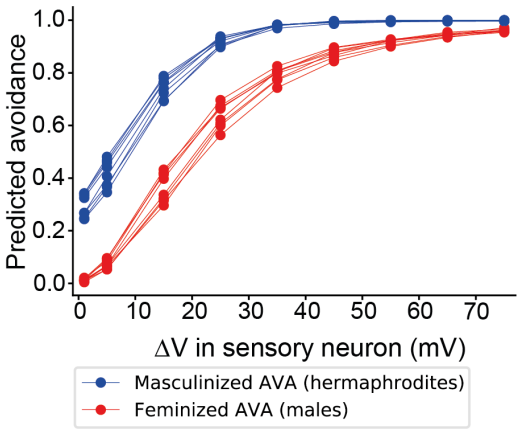

D

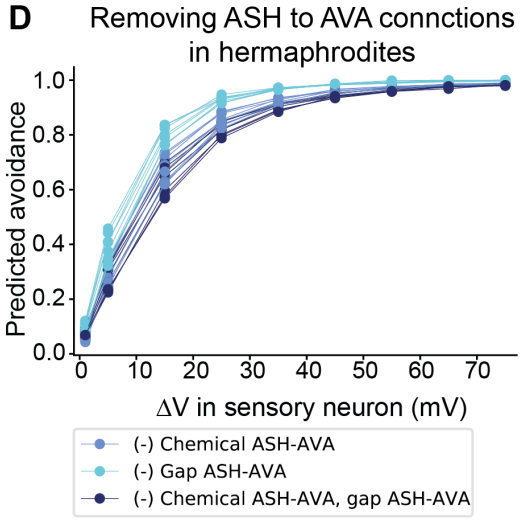

E

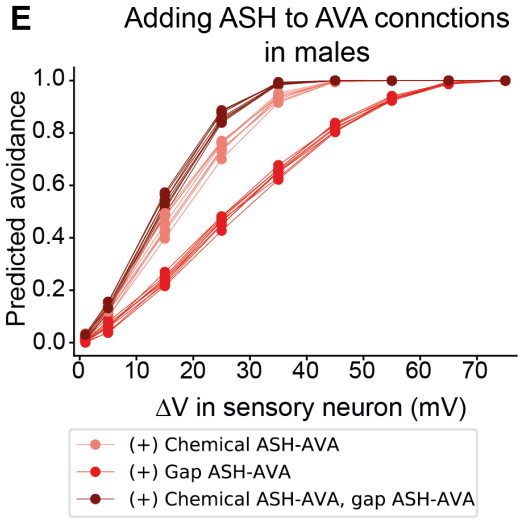

Figure S4. Excluding ASH-AVB, additional inhibitory connections have a minimal effect on the network performance, Related to Figures 3, 5 and 6

(A) Parameter combinations that met two sets of conditions; behavioral and physiological, divided to polarity configurations. Each row represents different combination of excitation and inhibition in the following connections: ASH-AVB, AVB-AVA, A-B, B-A (overall 16 options). Physiological conditions were tested only for the hermaphrodites' connectivity. Additional inhibitory connections (aside from ASH-AVB, which remained essential) have a minimal effect on the number of appropriate sets. (B-E) Computational model predictions of the escape response in worms with connectivity perturbations, using different polarity configurations that met all conditions. The polarity configurations include an inhibitory connection between ASH-AVB, and all of the combinations of inhibition and excitation of the following connections: AVB-AVA, A-B, B-A, a total of eight configurations. x axis, voltage increase in the sensory neuron following the stimulus (see Methods). y axis, predicted avoidance averaged over the appropriate sets, separately for each polarity configuration. (B) Computational model predictions of the escape response in worms with feminized or masculinized ASH. All connections of ASH are sex-switched. Backward movement is predicted to increase in ASH-feminized males, and decrease in ASH-masculinized hermaphrodites in all polarity configurations. (C) Computational model predictions of the escape response in worms with feminized or masculinized AVA. All connections of AVA are sex-switched. In all polarity configurations, backward movement is predicted to increase in AVA-feminized males, yet in AVA-masculinized hermaphrodites, the avoidance is not significantly affected. (D) Model predictions of the escape response in hermaphrodites without ASH-AVA connections (chemical, electrical, or both). Backward movement is predicted to slightly decrease in hermaphrodites without ASH-AVA connections in all polarity configurations. (E) Model predictions of the escape response in males with additional connections between ASH and AVA (chemical, electrical, or both). Regardless of the polarity, backward movement is predicted to significantly increase in males with ASH-AVA connections.

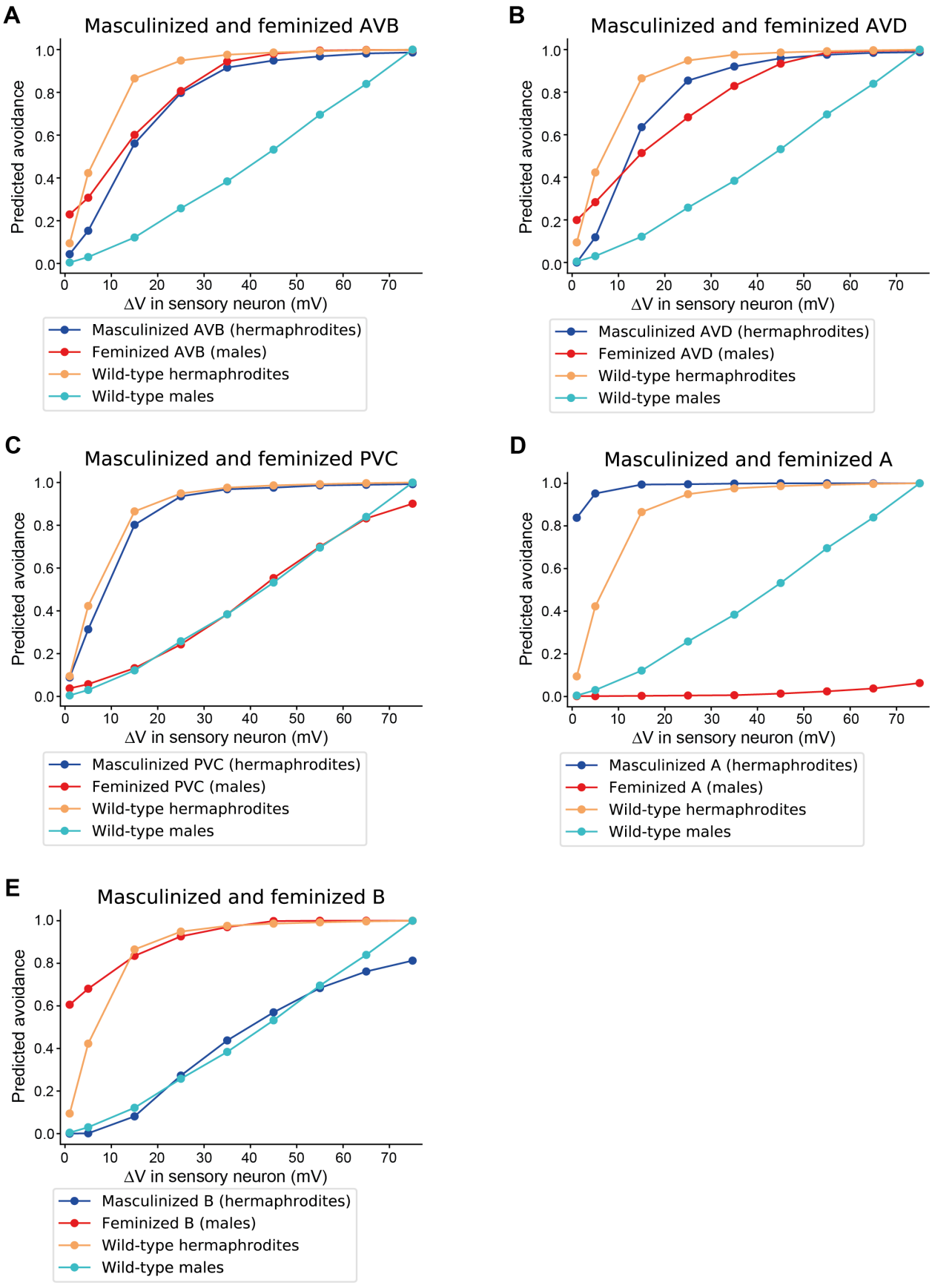
A
Masculinized and feminized AVB
Predicted avoidance
ΔV in sensory neuron (mV)
Masculinized AVB (hermaphrodites)
Feminized AVB (males)
Wild-type hermaphrodites
Wild-type males
B
Masculinized and feminized AVD
Predicted avoidance
ΔV in sensory neuron (mV)
Masculinized AVD (hermaphrodites)
Feminized AVD (males)
Wild-type hermaphrodites
Wild-type males
C
Masculinized and feminized PVC
Predicted avoidance
ΔV in sensory neuron (mV)
Masculinized PVC (hermaphrodites)
Feminized PVC (males)
Wild-type hermaphrodites
Wild-type males
D
Masculinized and feminized A
Predicted avoidance
ΔV in sensory neuron (mV)
Masculinized A (hermaphrodites)
Feminized A (males)
Wild-type hermaphrodites
Wild-type males
E
Masculinized and feminized B
Predicted avoidance
ΔV in sensory neuron (mV)
Masculinized B (hermaphrodites)
Feminized B (males)
Wild-type hermaphrodites
Wild-type males

Figure S5. Masculinizing and feminizing cells of the circuit have different behavioral effects, Related to Figure 5

(A-E) Computational model predictions of backward movement in wild-type animals and animals with one feminized or masculinized cell. x axis, voltage increase in the sensory neuron following the stimulus (see Methods). y axis, predicted avoidance averaged over the appropriate sets. (A) Feminized and masculinized AVB neurons (all connections of AVB are sex-switched). Backward movement is predicted to significantly increase in feminized males. In masculinized hermaphrodites, the avoidance is not significantly affected. (B) Feminized and masculinized AVD neurons. Backward movement is predicted to increase in feminized males and insignificantly decrease in masculinized hermaphrodites. (C) Feminized and masculinized PVC neurons. Switching the connections of PVC did not result in a behavioral change for either sex. (D) Feminized and masculinized A neurons. Backward movement is predicted to decrease in feminized males below that predicted for wild-type males. Accordingly, in masculinized hermaphrodites, the avoidance slightly increased. (E) Feminized and masculinized B neurons. Backward movement is predicted to significantly increase in feminized males and significantly decrease in masculinized hermaphrodites.

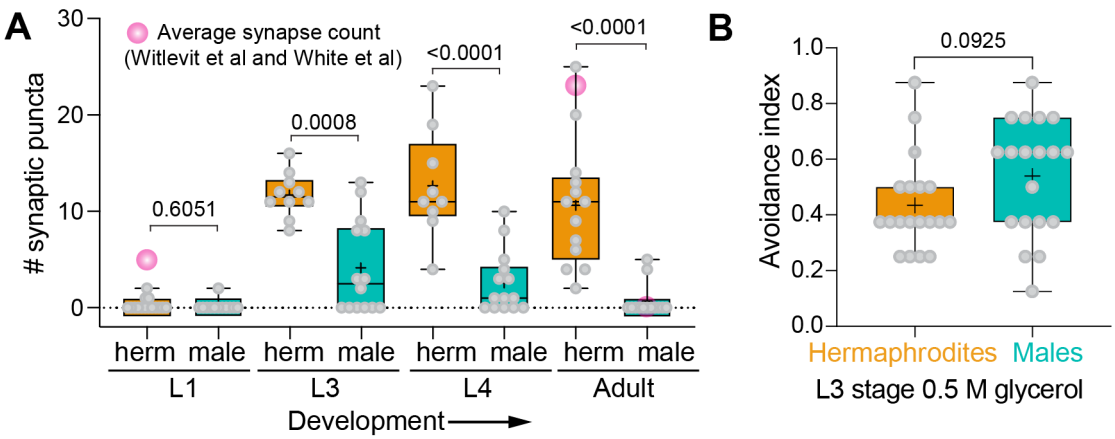

Figure S6. Temporal analysis of the ASH-AVA connection and the avoidance responses of juvenile animals, Related to Figure 5

(A) Quantification of ASH-AVA iBLINC GFP puncta in hermaphrodites and males at four developmental stages. n = 9-15 for each group. Pink circles represent the average synapse count from electron microscopy reconstructions for hermaphrodites[S1, S2] and males[S3]. Male electron-microscopy data exists only for the adult. (B) Quantification of the behavioral responses of juvenile L3 animals to aversive stimuli. The avoidance index in the tail-drop assay is calculated as in Figure 1. All plots are box and whiskers plots, vertical lines represent the medians and "+" are the means. We performed a Mann-Whitney test for all comparisons.

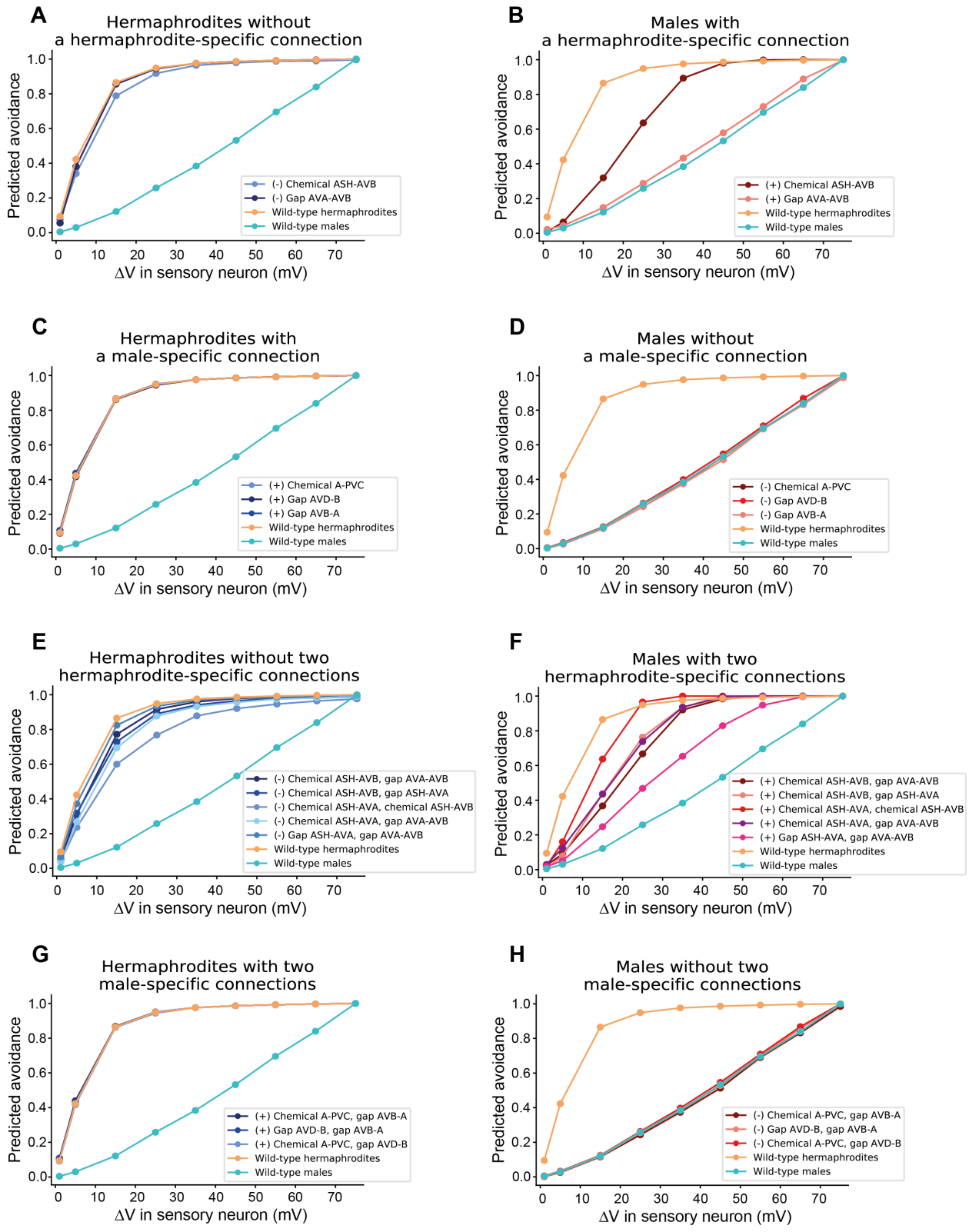
A
Hermaphrodites without
a hermaphrodite-specific connection
Predicted avoidance
ΔV in sensory neuron (mV)
(-) Chemical ASH-AVB
(-) Gap AVA-AVB
Wild-type hermaphrodites
Wild-type males
B
Males with
a hermaphrodite-specific connection
(+) Chemical ASH-AVB
(+) Gap AVA-AVB
C
Hermaphrodites with
a male-specific connection
(+) Chemical A-PVC
(+) Gap AVD-B
(+) Gap AVB-A
D
Males without
a male-specific connection
(-) Chemical A-PVC
(-) Gap AVD-B
(-) Gap AVB-A
E
Hermaphrodites without two
hermaphrodite-specific connections
(-) Chemical ASH-AVB, gap AVA-AVB
(-) Chemical ASH-AVB, gap ASH-AVA
(-) Chemical ASH-AVA, chemical ASH-AVB
(-) Chemical ASH-AVA, gap AVA-AVB
(-) Gap ASH-AVA, gap AVA-AVB
F
Males with two
hermaphrodite-specific connections
(+) Chemical ASH-AVB, gap AVA-AVB
(+) Chemical ASH-AVB, gap ASH-AVA
(+) Chemical ASH-AVA, chemical ASH-AVB
(+) Chemical ASH-AVA, gap AVA-AVB
(+) Gap ASH-AVA, gap AVA-AVB
G
Hermaphrodites with two
male-specific connections
(+) Chemical A-PVC, gap AVB-A
(+) Gap AVD-B, gap AVB-A
(+) Chemical A-PVC, gap AVD-B
H
Males without two
male-specific connections
(-) Chemical A-PVC, gap AVB-A
(-) Gap AVD-B, gap AVB-A
(-) Chemical A-PVC, gap AVD-B

Figure S7. Rewiring a single connection or two connections simultaneously had a minor effect on hermaphrodites but significantly changed male behavior, Related to Figure 6

(A-D) Computational model predictions of backward movement in wild-type animals and in animals with one connection feminized or masculinized. (A) Eliminating a single hermaphrodite-specific connection in hermaphrodites did not result in a behavioral change. (B) Inserting a single hermaphrodite-specific connection into males resulted in behavioral changes. The chemical connection of ASH to AVB increased the males' backward movement, while the gap junction between AVA to AVB did not significantly affect their behavior. (C) In hermaphrodites, inserting a single male-specific connection did not affect their behavior. (D) In males, removing a single male-specific connection did not affect their behavior. (E-H) Computational model predictions of backward movement in wild-type animals and in animals with two connections feminized or masculinized simultaneously. (E) In hermaphrodites, removing simultaneously two hermaphrodite-specific connections resulted in a slight, insignificant change in their response. (F) In males, inserting simultaneously any two hermaphrodite-specific connections resulted in an increased avoidance. (G) In hermaphrodites, inserting two male-specific connections did not affect their behavior. (H) In males, removing two male-specific connections did not affect their behavior. (A-H) x axis, voltage increase in the sensory neuron following the stimulus (see Methods). y axis, predicted avoidance averaged over the appropriate sets.

Supplemental References

S1. White, J.G., Southgate, E., Thomson, J.N., and Brenner, S. (1986). The structure of the nervous system of Caenorhabditis elegans. Philos. Trans. R. Soc. Lond. B Biol. Sci *314*, 1–340.

S2. Witvliet, D., Mulcahy, B., Mitchell, J.K., Meirovitch, Y., Berger, D.R., Wu, Y., Liu, Y., Koh, W.X., Parvathala, R., Holmyard, D., et al. (2021). Connectomes across development reveal principles of brain maturation. Nature *596*, 257–261.

S3. Cook, S.J., Jarrell, T.A., Brittin, C.A., Wang, Y., Bloniarz, A.E., Yakovlev, M.A., Nguyen, K.C.Q., Tang, L.T.-H., Bayer, E.A., Duerr, J.S., et al. (2019). Whole-animal connectomes of both Caenorhabditis elegans sexes. Nature *571*, 63–71.